Title

Surface Damage Influences the JKR Contact Mechanics of Glassy Low-Molecular-Weight Polystyrene Films

Journal

Langmuir, 35(48)

ISSN

0743-7463

Authors

Degen, George D
Cristiani, Thomas R
Cadirov, Nicholas
et al.

Publication Date

2019-12-03

DOI

10.1021/acs.langmuir.9b02037

Peer reviewed

LANGMUIR Article
Cite This: Langmuir 2019, 35, 15674−15680
pubs.acs.org/Langmuir

Surface Damage Influences the JKR Contact Mechanics of Glassy Low-Molecular-Weight Polystyrene Films

George D. Degen,*[,†] Thomas R. Cristiani,[†] Nicholas Cadirov,[†] Roberto C. Andresen Eguiluz,[†,§] Kai Kristiansen,[†] Angela A. Pitenis,[‡] and Jacob N. Israelachvili[†,‡]

[†]Department of Chemical Engineering and [‡]Materials Department, University of California, Santa Barbara, California 93106, United States

Supporting Information

ABSTRACT: Using a surface forces apparatus (SFA), we quantitatively study the influence of surface damage on the contact mechanics of self-mated glassy polystyrene (PS) films. We use the SFA to measure the contact radius, surface profile, and normal force between the films, including the adhesion force. The molecular weight (MW) of the polymer influences the repeatability of the adhesion measurements and the effective surface energy calculated using the Johnson−Kendall−Roberts (JKR) theory. For low-MW PS (MW = 2.33 kDa), the effective surface energy increases over repeated adhesion cycles as the films become progressively damaged. For high-MW PS (MW = 280 kDa), the effective surface energy is constant over repeated adhesion cycles, but hysteresis is still present, manifested in a smaller contact radius during compression of the surfaces than during separation. Our results demonstrate that while the JKR theory is appropriate for describing the contact mechanics of glassy polymer thin films on layered elastic substrates, the contact mechanics of low-MW polymer films can be complicated by surface damage to the films.

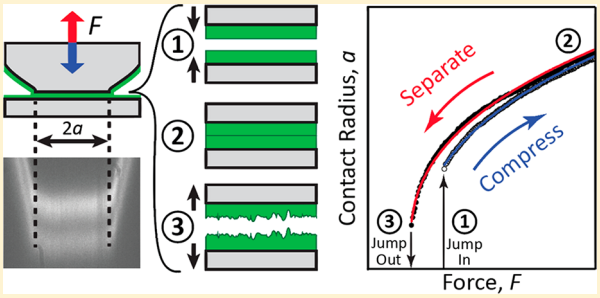

INTRODUCTION

Surface energy is an important property governing the adhesion and cohesion of polymer materials. However, many methods used to measure this quantity have limitations. Contact angles can be used to calculate surface energies indirectly, but these methods can be inaccurate and model-dependent[1] and cannot account for the effects of confinement. Macroscopic adhesion tests such as peel tests can require relatively large amounts of material, can make the identification of impurities/defects difficult, and can yield large, non-thermodynamic fracture energies,[1] often due to crazing.[2] Therefore, controlled contact mechanics studies (e.g., using a surface force apparatus (SFA), JKR apparatus, or atomic force microscope (AFM)) are preferable alternatives for measuring the surface energy of solid polymer materials.

Contact mechanics studies of adhesive, elastically deformable surfaces usually employ the Johnson−Kendall−Roberts (JKR) theory.[3] The theory relates the force (F_{ad}) required to separate two adhering elastic spheres of the same material and radii R_1 and R_2 to the surface energy (γ)

$$F_{ad} = -3\pi R\gamma \quad (1)$$

where $R = R_1R_2/(R_1 + R_2)$. The theory also relates the contact radius (a) to the normal force (F)

$$a^3 = (3R/4E^*)(F + 6\pi R\gamma \pm (12\pi R\gamma F + (6\pi R\gamma)^2)^{1/2}) \quad (2)$$

where the contact modulus E^* is related to the elastic moduli (E_1 and E_2) and Poisson's ratios (ν_1 and ν_2) of the contacting materials by $1/E^* = (1 - \nu_1^2)/E_1 + (1 - \nu_2^2)/E_2$. For layered materials, an effective contact modulus (E^*_{eff}) is used. Thus, two ways to calculate γ are by measuring F_{ad} and applying eq 1 or by measuring a as a function of F and fitting eq 2 with γ as a fitting parameter.

The JKR theory has been extensively used to calculate the surface energy of polymers in contact mechanics studies of thin polymer films on elastic substrates.[4,5] Although solid polymers are typically rigid and can have nonlinear elasticity,[6] both of which make JKR measurements of bulk polymer materials difficult, thin polymer films on elastic substrates generally satisfy the assumptions of the JKR theory. Specifically, many contact mechanics studies have involved thin films of polystyrene (PS).[1,4,7−13] However, the adhesion measured between polymer films often exceeds the value predicted from thermodynamics, and eq 2 often predicts a during compression of the surfaces (increasing F and a) but not during separation (decreasing F and a). When such deviations from the JKR theory occur, called contact or adhesion hysteresis, the surface

Special Issue: Intermolecular Forces and Interfacial Science

Received: July 2, 2019
Revised: September 29, 2019
Published: September 30, 2019

DOI: 10.1021/acs.langmuir.9b02037
Langmuir 2019, 35, 15674−15680

energy (γ) in eqs 1 and 2 is replaced with the effective surface energy (γ_{eff}).

Contact hysteresis is often attributed to energy dissipation due to viscoelasticity of the substrates underlying the polymer films and/or polymer diffusion across the interface (interdiffusion).[14] Interdiffusion can increase F_{ad} and γ_{eff} by increasing the real area of contact and therefore the number of bonds across the interface.[6] Because the JKR theory assumes contact between infinitely smooth surfaces, if the real area of contact is greater than the nominal area of contact, then the measured F_{ad} will be larger than the value of F_{ad} predicted by eq 1. Interdiffusion occurs readily for contacting polymer melts[14] or grafted brushes into a melt[15] or network,[16] but the extent to which interdiffusion can occur for polymers at temperatures below the glass transition temperature ($T < T_g$) is unclear. Self-diffusion of glassy polymers has been thought to be unmeasurably slow.[17] However, it has been shown that the T_g of PS near a solid−vapor interface can be lower than the bulk T_g,[18,19] which corresponds to an increase in molecular mobility at the surface.[20] Simulations confirm the enhanced mobility of polymer chains at a free interface and correlate this mobility to an interfacial region of decreased polymer density.[21] Therefore, an interface between two such regions (e.g., between self-mated PS films) is expected to be fundamentally different from bulk PS. Polymer chains at the interface between self-mated films may be more mobile than chains in the bulk and therefore better able to interdiffuse. Furthermore, limited interdiffusion between self-mated films (here called interdigitation) and penetration by as few as one to two monomer units of polymer chains into the opposite film is sufficient to increase adhesion.[7] Such interdigitation corresponds to penetration distances (<5 Å) that are difficult to measure directly: neutron scattering is often used to measure interdiffusion, but small interfacial widths can be difficult to distinguish from interfacial roughness.[16] Nevertheless, interdigitation has been proposed to contribute to adhesion and contact hysteresis of glassy PS.[7,8,13,22,23]

Contact mechanics of polymer films can also be influenced by surface damage, including polymer chains pulled out of the film, cohesive failure within the film, or film detachment from the underlying substrate. Previous studies have described damage of films of low-MW PS (<3 kDa) in air[8−11,13] and films of much higher MW PS (1000 kDa) in water.[12] However, the studies did not explore the impact of damage on the contact mechanics of the films, including adhesion and contact radius.

Here, we use a surface forces apparatus (SFA) to simultaneously measure the normal force and contact radius during cycles of compression, separation, and jump from contact (here called adhesion cycles) of self-mated films of low-MW PS (MW = 2.33 kDa) and high-MW PS (MW = 280 kDa). We show that damage to the low-MW PS films occurs as early as the first adhesion cycle. This damage is correlated to changes in the measured forces and contact radii. In particular, the adhesion force can increase by up to 100% over repeated adhesion cycles. In contrast, films of high-MW PS (MW = 280 kDa) remain undamaged over >100 adhesion cycles, yielding consistent forces and contact radii. To explain our results, we propose that entanglements in the high-MW PS films enable the films to resist damage and that the low-MW PS films are susceptible to damage due to their inability to form entanglements.

EXPERIMENTAL SECTION

Normal forces between self-mated PS films deposited on mica were measured using a surface forces apparatus (SFA), as described in detail elsewhere.[24] Briefly, molecularly smooth mica sheets of thickness 3−5 μm were cleaved and then coated on one side with a reflective silver layer of thickness 50 nm via thermal evaporation. Mica surfaces were prepared using established methods to avoid contamination.[25] The silver-coated mica was then glued (EPON 1004F, Miller-Stephenson Chemical or NOA81, Norland Products) onto semicylindrical fused silica disks (radius of curvature 2 cm) with the mica surface exposed. For each experiment, two such surfaces were prepared. Films of PS of the same MW were then deposited on each mica surface. Two molecular weights of PS were used: low-MW PS (MW = 2.33 kDa, T_g = 69 °C)[9] and high-MW PS (MW = 280 kDa, T_g = 106 °C)[9] (Sigma-Aldrich). Solid PS samples were dissolved at 5 wt % in toluene and spin-coated onto the mica surfaces. The surfaces were then dried in active vacuum for >12 h at 22 °C.

White light multiple beam interferometry was used to measure the distance between the surfaces. Because the refractive index of PS (1.5)[26] is close to the refractive index of mica (1.6)[27] over the wavelength range used for the analysis (∼500−600 nm), the combined mica/PS thickness was calculated from the interference fringes by assuming a single refractive index equal to the refractive index of mica and assuming uniform PS films of equal thickness. The mica thickness, measured from contact between bare mica surfaces, was subtracted from the mica/PS thickness to yield the PS film thickness (low-MW PS: 300−400 nm, high-MW PS: 750−800 nm). The interference fringes also yielded the average radius of curvature (R) of the contact region, as described further in Supporting Information S1. Experiments were conducted at 22 ± 1 °C, well below the bulk T_g of the PS samples. We note that these film thicknesses are well above the film thickness below which the bulk T_g of polystyrene has been observed to decrease (∼100 nm).[28]

The surfaces were arranged in a crossed-cylinder configuration, geometrically equivalent to contact between a spherical surface of radius R and a flat surface and therefore described by the JKR theory. The crossed cylinder configuration is preferable to sphere-on-flat and flat-on-flat configurations for several reasons: (i) mica sheets can be glued onto a cylinder without wrinkling or creasing (unlike mica on a spherical surface); (ii) crossed cylinders yield a single circular contact, enabling easy alignment of the surfaces (unlike flat-on-flat); and (iii) proper translation of one surface results in contact between previously uncontacted regions on each surface (unlike sphere-on-flat and flat-on-flat).

To measure the normal force (F) between the surfaces, one of the surfaces was suspended on a double cantilever spring (k = 30−40 kN/m). Deflections of the spring were converted to force with Hooke's law. For the force−distance profiles shown here, the separation distance corresponds to the distance between the contacting PS films. Adhesion cycles (approach, jump into contact, compression, separation, and jump from contact) were performed using a motorized micrometer to move one of the surfaces at constant velocity (6−17 nm/s) and corresponding constant compression and separation rate (0.2−0.5 mN/s) to an average maximum compression of F = 15−50 mN. The adhesion force (F_{ad}) was the force required to separate the surfaces from contact. The value of R changed over the course of an experiment (Figure S1), likely due to viscoelastic deformations of the glue layer beneath the mica. Equation 1 gives F_{ad} proportional to R, and since F_{ad} and R were directly measured for each adhesion cycle, γ_{eff} calculated with eq 1 was independent of the change in R.

A MATLAB script was written to extract the radius of the contact area (a) from the interference fringes. A two-parameter least-squares regression was used to fit eq 2 to plots of a vs F by varying γ_{eff} and E^*_{eff} of the layered surfaces. R was measured for each adhesion cycle as described above and was therefore not a fitting parameter. Fits were performed over three force ranges: F = 0−10, 0−20, and 0−30 mN. Negative (tensile) forces were excluded from the fitting ranges for separation to match the fitting ranges for compression.

DOI: 10.1021/acs.langmuir.9b02037
Langmuir 2019, 35, 15674−15680

The JKR theory is considered to be valid for symmetric surfaces when a dimensionless number called the Tabor parameter $\mu = (4R\gamma^2/E^{*2}z_0^3)^{1/3}$ exceeds 5, where z_0 is the equilibrium separation of the surfaces.[29] Another model describing the contact mechanics of adhesive materials, the Derjaguin–Muller–Toporov (DMT) model,[30] becomes valid as the Tabor parameter approaches zero. Taking z_0 = 0.3 nm (atomic contact) and representative values from our experiments (E^*_{eff} = 20 GPa, R = 2 cm, and γ = 40 mJ/m^2) yields μ = 20, indicating that the JKR theory is applicable for our experimental system. We note that the use of the JKR theory to describe SFA measurements of polymer films has extensive precedent in the literature but that in general the JKR theory cannot be assumed to be valid, since E^*_{eff} and γ can vary widely with the choice of surfaces. Therefore, the Tabor parameter should be calculated for each experimental system to determine whether the JKR theory is applicable.

Another dimensionless number, the adhesion parameter $\alpha = (4\gamma R^2(1-\nu^2)/Eh^3)^{1/2}$, corresponds to the deviation from the JKR theory resulting from the use of layered materials in the SFA[31] rather than homogeneous and isotropic materials. Here, E, ν, and h are the Young's modulus, Poisson ratio, and thickness, respectively, of the mica. Taking γ = 40 mJ/m^2, R = 2 cm, E = 70 GPa,[32] ν = 0.25,[33] and h = 4 μm yields α = 4, indicating that eq 1 will underpredict γ by 10–20%.[31] We assume that the polystyrene film determines the surface energy but does not otherwise impact the contact mechanics of the layered system because it is thin relative to the mica and glue layers, a common assumption in studies of polymer films on deformable substrates.[4] Quantifying any additional influence of the polymer film on the calculation and interpretation of α is beyond the scope of this work. For the present study, the values of the Tabor parameter and the adhesion parameter suggest that the JKR theory is appropriate for our experimental system.

RESULTS AND DISCUSSION

The measured adhesion force (F_{ad}) and effective surface energy (γ_{eff}) varied over repeated adhesion cycles of films of low-MW PS. Figure 1 shows γ_{eff} of the low-MW PS films

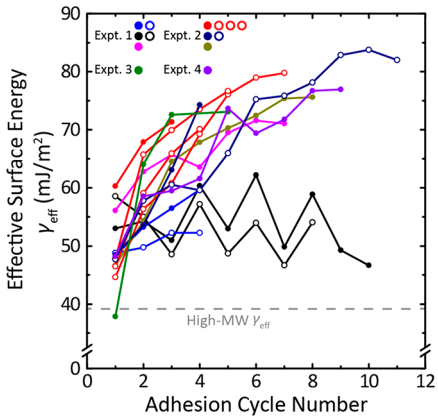

Figure 1. Plots of effective surface energy (γ_{eff}) vs adhesion cycle number for self-mated low-MW PS films. γ_{eff} measured for high-MW PS films is shown for reference (dashed gray line).

calculated from F_{ad} with eq 1 and plotted as a function of the adhesion cycle number. The results of four independent experiments are shown, each with a different pair of mica surfaces. Experiments involved sequential adhesion cycles at the same contact location (closed circles). The waiting time between adhesion cycles was minimized (t_{relax} < 60 s). Subsequently, the surfaces were held out of contact (t_{relax} > 8 h). After this relaxation period, sequential adhesion cycles were again conducted at the same contact location (open circles). γ_{eff} generally increased over repeated adhesion cycles by up to 100%. After the relaxation period, γ_{eff} returned to approximately the initial value and then increased on subsequent adhesion cycles. An example of the reversible change in γ_{eff} for a single experiment is shown in Figure S2.

We hypothesize that the change in γ_{eff} measured for low-MW PS films results from surface damage of the films. Upon jump from adhesive contact, discontinuities appeared in the interference fringes that gradually faded over the course of minutes with the surfaces out of contact (Figure S3). We attribute these discontinuities to damage of the films. Consistent with this interpretation, measured forces and contact radii changed after the first adhesion cycle. Figure 2A shows plots of the normal force divided by the radius of

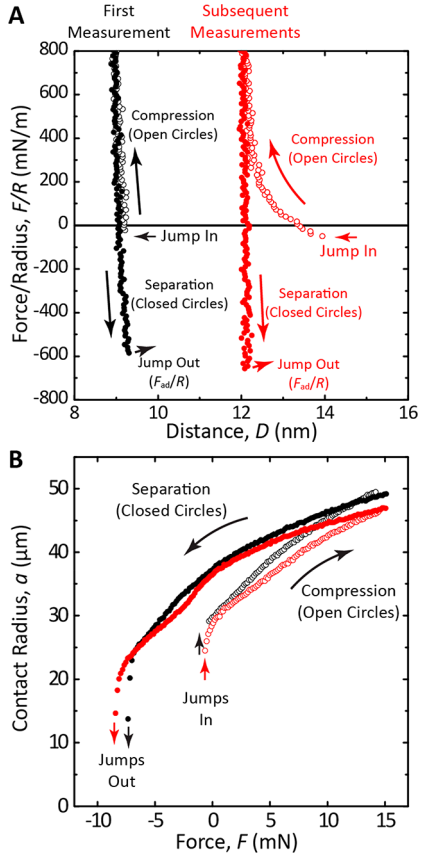

Figure 2. (A) Plots of normal force divided by the radius of curvature of the surfaces (F/R) vs surface separation distance (D) for self-mated low-MW PS films. (B) Corresponding plots of contact radius (a) vs normal force (F) between the surfaces.

curvature (F/R) vs the surface separation distance (D) for self-mated low-MW PS films. Black circles show an adhesion cycle in which neither film had been previously contacted at that location. As the surface are compressed (open circles), F increases to >800 mN/m while D decreases by <1 nm. In contrast, red circles show a subsequent adhesion cycle in which D decreases by ∼2 nm as F increases to >800 mN/m, an increase in the range of repulsion. The value of D at F = 800 mN/m also increases by ∼3 nm from the first to the second adhesion cycle. Since D = 0 corresponds to contact between a specific location on each PS film, changing the contact location results in nonzero values of D due to variations in film thickness. For a fixed contact location, changes in D indicate

DOI: 10.1021/acs.langmuir.9b02037
Langmuir 2019, 35, 15674–15680

changes in film thickness. Here, the range of repulsion and film thickness increase from the first to the second adhesion cycle, consistent with damage occurring during the first cycle. The range of repulsion and compressed film thickness returned to the initial values after the surfaces were held out of contact (t_{relax} > 8 h) (Figure S4). Damage may heal in a process similar to craze healing,[34] which can be enhanced by an elevated concentration of chain ends at a fractured interface due to chain scission.[35]

Measured contact radii further suggest that damage occurs during the first adhesion cycle. Figure 2B shows plots of the contact radius (a) vs the normal force (F) between the surfaces for the same adhesion cycles shown in Figure 2A. Values of a measured in the first adhesion cycle (black circles) were larger than values of a measured in subsequent adhesion cycles (red circles) during both compression (open circles) and separation for $F > -5$ mN (closed circles). The decrease in a after the first adhesion cycle is consistent with damage occurring during the cycle. Damaged films may require larger compressive forces than undamaged films to reach the same nominal contact area due to the need to compress surface asperities on the damaged films.

Interestingly, the damage was also correlated with increasing F_{ad} and γ_{eff} (Figure 1), which we propose results from an increase in the real contact area between the films. A previous study showed that surface roughness can increase the adhesion between polymer surfaces by increasing the real contact area.[36] In our experiments, damage increases the surface roughness and may similarly increase the real contact area. Damage may also increase the percentage of chain ends at the interface due to chain scission,[35] which can promote interdigitation of the films and thereby increase the real contact area and adhesion.[8] It has also recently been shown that plastic deformation can increase polymer mobility, resulting in increased interdigitation and adhesion between glassy polymer films.[37] As a result, surface damage to low-MW PS films may result in the seemingly contradictory effects of increasing the adhesion force while also increasing the range of repulsion and decreasing the nominal contact area.

Increased waiting time at maximum compression (t_{wait}) resulted in irreversible damage to the low-MW PS films. For t_{wait} = 60 s, stick−slip detachment was observed (Figure S5), consistent with previous studies of PS adhesion to mica.[13] Longer waiting times (t_{wait} = 10, 30, and 60 min) resulted in substantially more damage to the films, including cohesive failure within the films and material transfer between films (Figure S6). The damage dramatically altered the interference fringes and precluded further accurate measurements. Such catastrophic damage did not heal after the surfaces were held out of contact, and therefore no further adhesion cycles were performed at such irreversibly damaged contact locations.

Damage to the low-MW PS films also occurred at the edge of the contact region during adhesion cycles. Figure 3 shows plots of a vs F for sequential adhesion cycles of low-MW PS films. Black circles show an adhesion cycle in which neither film had been previously contacted at that location. Open circles correspond to compression of the surfaces; closed circles correspond to separation. Blue circles show a vs F for a subsequent adhesion cycle in which the surfaces were compressed to a larger maximum force than in the first adhesion cycle. For F = 15−20 mN during the second compression, a was approximately constant, suggesting that the advancing contact edge was pinned. Pinning during the second

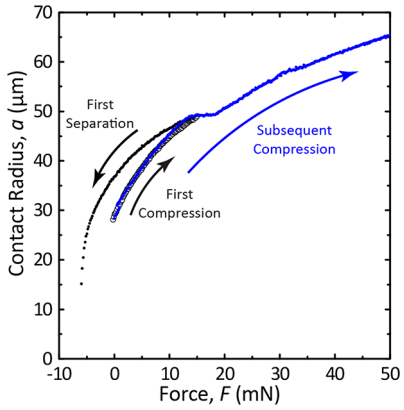

Figure 3. Plots of contact radius (a) vs normal force (F) for self-mated low-MW PS films.

compression occurred at the contact radius corresponding to maximum compression during the first adhesion cycle (a = 48 μm at F = 15 mN). Therefore, damage occurring at the contact edge during the first adhesion cycle may have pinned the advancing contact edge during the second adhesion cycle due to the need to compress asperities before further increases in contact area. Evidence of edge damage sometimes appeared in the interference fringes (Figure S7) for sufficiently large asperities (1 to 2 nm). Evidence of edge damage disappeared after the surfaces were held out of contact (t_{relax} > 8 h).

Edge damage may result from enhanced interdigitation of polymers at the contact edge. During the transition from compression to separation of the surfaces in an adhesion cycle, backlash of the motorized micrometer typically resulted in a wait time of ∼20 s during which the surfaces were stationary. This wait time may have enabled increased amounts of interdigitation to occur between the films. Interdigitation due to enhanced polymer chain mobility at the polymer−vapor interface has previously been proposed to occur for PS at temperatures as low as 50 °C below the bulk T_g[23] and could therefore be expected to occur for the low-MW PS in this work ($T_g - T$ = 47 °C), especially since the low-MW PS has a relatively large concentration of chain ends at the interface, which are known to enhance interdigitation.[8] Although interdigitation would seemingly occur throughout the entire contact area during an adhesion cycle, compressive stress can increase the viscosity[38] and relaxation time(s) of polystyrene.[39−41] The JKR theory predicts the stress distribution across the contact

$$P = (2E^*a/\pi R)(1 - r^2/a^2)^{1/2} - ((4E^*\gamma/\pi a)/(1 - r^2/a^2))^{1/2} \quad (3)$$

where r is the radial distance from the center of contact, plotted in Figure S8. Equation 3 shows that the maximum compressive stress occurs at the center of the contact area and that a transition from compressive to tensile stress occurs at the edge of the contact area. As a result, interdigitation may be enhanced at the edge of the contact relative to the interior of the contact, where compressive stress may reduce the molecular mobility and limit interdigitation. Therefore, enhanced interdigitation at the contact edge during the wait time at maximum compression discussed above may result in damage upon separation of the surfaces.

In contrast with the low-MW PS films, high-MW PS films resisted damage during adhesion cycles and yielded consistent forces and contact radii. Figure 4A shows a representative

DOI: 10.1021/acs.langmuir.9b02037
Langmuir 2019, 35, 15674−15680

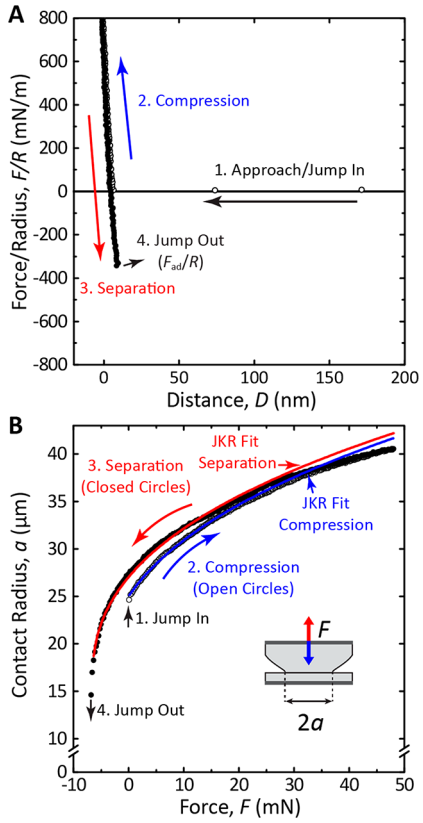

Figure 4. (A) Plots of normal force divided by the radius of curvature of the surfaces (F/R) vs surface separation distance (D) for self-mated high-MW PS films. (B) Corresponding plots of contact radius (a) vs normal force (F). Blue and red lines show fits using eq 2 for compression and separation of the surfaces, respectively.

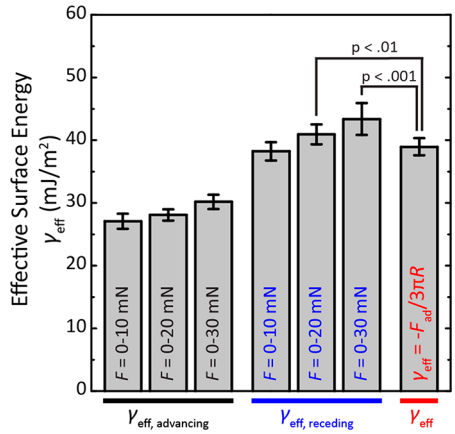

Figure 5. Effective surface energies from fitting eq 2 for the compression ($\gamma_{eff,advancing}$) and separation ($\gamma_{eff,receding}$) of high-MW PS films. γ_{eff} calculated from F_{ad} with eq 1 is shown for comparison.

force−distance plot for an adhesion cycle involving self-mated high-MW PS films. Open circles correspond to approach and compression of the surfaces; closed circles correspond to separation and jump from contact. Figure 4B shows a plot of a vs F for the same adhesion cycle shown in Figure 4A. Open circles correspond to compression; closed circles correspond to separation. Equation 2 was fit to the plots of a vs F for compression (blue line) and separation (red line).

Effective surface energies and contact moduli were approximately constant over repeated adhesion cycles (Figure S9) and were consistent with previous measurements of PS surface energy.[1,4,42] Figure 5 shows effective surface energies of the high-MW PS films calculated by fitting eq 2 to plots of a vs F for compression ($\gamma_{eff,\ advancing}$) and separation ($\gamma_{eff,receding}$) over the force ranges F = 0−10, 0−20, and 0−30 mN. γ_{eff} calculated from F_{ad} with eq 1 is shown for comparison. Hysteresis was observed: $\gamma_{eff,\ advancing}$ was lower than $\gamma_{eff,receding}$ for all fitting ranges. We attribute the hysteresis to viscoelastic energy dissipation during the deformation of the glue layer. Complementary experiments of contact between bare mica surfaces showed dramatic hysteresis (Figure S10), consistent with previous SFA studies.[31,43] The surface energy of mica is higher than the surface energy of PS, resulting in greater deformation of the surfaces, thus magnifying the effects of viscoelastic energy dissipation. Unlike for the low-MW PS, interdigitation is not expected to occur for the high-MW PS ($T_g - T$ = 84 °C). Therefore, the dramatic hysteresis measured for contact between bare mica surfaces suggests viscoelastic energy dissipation as the principal contributor to the hysteresis of the high-MW PS films.

The values of γ_{eff} and E^*_{eff} calculated with eq 2 depended on the fitting range. The fit over F = 0−10 mN yielded $\gamma_{eff,receding}$ in good agreement with γ_{eff} from eq 1. Fits over larger force ranges (F = 0−20 and 0−30 mN) yielded $\gamma_{eff,receding}$ greater than γ_{eff} from eq 1. The fit over F = 0−10 mN yielded a better prediction of a at tensile forces (F < 0) than the fits over F = 0−20 and 0−30 mN but a worse prediction at the largest compressive forces (Figure S11). All fits overpredicted a for F < 0, consistent with a previous study.[42] The value of E^*_{eff} also depended on the fitting range (Figure S12), with an approximately 20% difference between the minimum ($E^*_{eff,advancing}$ for F = 0−10 mN) and maximum ($E^*_{eff,receding}$ for F = 0−30 mN) values. The value of E^*_{eff} increased with increasing maximum force included in the fitting range (i.e., from F = 0−10 to F = 0−30 mN), consistent with an increasing influence of the stiff underlying silica disks at increased indentation depths.[43] Calculations of γ_{eff} and E^*_{eff} with eq 2 were likely also influenced by the hysteresis discussed above.

The high-MW PS films resisted damage, and eqs 1 and 2 yielded consistent values of γ_{eff} and E^*_{eff}, even after >100 consecutive adhesion cycles. We propose that the difference in susceptibility to damage between low-MW and high-MW PS films can be explained by entanglement of the polymer chains in the high-MW PS films. Entanglements are defined as topological restrictions to polymer chain mobility caused by the inability of polymer chains to pass through one another without breaking.[44] Entangled polymer networks are characterized by the entanglement length (the average length of a macromolecule segment between neighboring entanglements) and by the corresponding entanglement molecular weight, M_e.[45] For polystyrene, M_e = 16.6 kDa.[26] Here, low-MW PS (MW = 2.33 kDa) is well below M_e and thus cannot form entanglements. In contrast, high-MW PS (MW = 280 kDa) is well above M_e and is therefore expected to be entangled. We propose that the lack of entanglement in films of low-MW PS makes the films susceptible to damage, and that entanglements in the high-MW PS films may strengthen film cohesion and prevent damage. Elevated adhesion forces resulting from interdigitation of low-MW PS as discussed above may also contribute to damage of the low-MW films.

DOI: 10.1021/acs.langmuir.9b02037
Langmuir 2019, 35, 15674−15680

CONCLUSIONS

We investigated the contact mechanics of self-mated glassy polystyrene films using a surface forces apparatus. Films of low-MW PS were susceptible to surface damage over repeated adhesion cycles, resulting in an increased effective surface energy and changes in the measured contact radii. The effects of damage were reversed after the surfaces were held out of contact. In contrast, films of high-MW PS films yielded consistent surface energies over repeated adhesion cycles. Viscoelastic energy dissipation was likely responsible for the hysteresis of the high-MW PS films. We propose that the susceptibility to damage of low-MW PS results from the inability of the polymer chains to form entanglements and that entanglements in the high-MW PS films prevent surface damage. The results suggest that films of polymers of molecular weight below M_e will in general be more susceptible to damage than films of polymers of molecular weight above M_e. A deeper understanding of the relationship between polymer entanglement and surface damage will require further contact mechanics studies of polymers of molecular weight at and around M_e.

ASSOCIATED CONTENT

Supporting Information

The Supporting Information is available free of charge on the ACS Publications website at DOI: 10.1021/acs.langmuir.9b02037.

Calculation of the average radius of curvature of the contact region; change in the average radius of curvature; increasing effective surface energy of low-MW PS films; discontinuities in the SFA interference fringes corresponding to surface damage; repulsion due to surface damage; stick−slip detachment of self-mated low-MW PS films; confocal microscopy images of damage to the low-MW PS films; interference fringes showing damage at the contact edge; stress distribution across the contact area given by eq 3; effective surface energy and combined modulus over repeated adhesion cycles; plot of contact radius vs normal force for contacting mica surfaces; fits of contact radius vs applied load using eq 2; fitting range influence on the effective contact moduli predicted by eq 2 for the compression and separation of high-MW PS films (PDF)

AUTHOR INFORMATION

ORCID

George D. Degen: 0000-0002-7386-506X
Thomas R. Cristiani: 0000-0003-3303-7865
Kai Kristiansen: 0000-0002-7555-9437
Jacob N. Israelachvili: 0000-0001-8915-8741

Present Address

[§]Materials Science and Engineering Department, University of California, Merced, California 95343, United States.

Notes

The authors declare no competing financial interest.

ACKNOWLEDGMENTS

G.D.D. was supported by the National Science Foundation Graduate Research Fellowship Program under grant no. 1650114. Any opinions, findings, and conclusions or recommendations expressed in this material are those of the authors and do not necessarily reflect the views of the National Science Foundation. Confocal microscopy images were taken in the University of California Santa Barbara (UCSB) nanofabrication facility, part of the NSF-funded National Nanotechnology Infrastructure Network (NNIN) network.

REFERENCES

(1) Mangipudi, V. S.; Tirrell, M. Contact-Mechanics-Based Studies of Adhesion between Polymers. *Rubber Chem. Technol.* **1998**, *71* (3), 407−448.

(2) Robertson, R. E. The Fracture Energy of Low Molecular Weight Fractions of Polystyrene. In *Toughness and Brittleness of Plastics*; UTC, 1976; Vol. *19*, pp 89−96.

(3) Israelachvili, J. N. *Intermolecular and Surface Forces*, 3rd ed.; Academic Press, 2011.

(4) Li, L.; Mangipudi, V. S.; Tirrell, M.; Pocius, A. V. Direct Measurement of Surface and Interfacial Energies of Glassy Polymers and Pdms. In *Fundamentals of Tribology and Bridging the Gap Between the Macro- and Micro/Nanoscales*; Springer: Dordrecht, The Netherlands, 2012; pp 305−329.

(5) Ruths, M. Characterization of Molecularly Thin Polymer Layers with the Surface Forces Apparatus (SFA). *Functional Polymer Films* **2011**, 745−769.

(6) Tirrell, M. Measurement of Interfacial Energy at Solid Polymer Surfaces. *Langmuir* **1996**, *12* (19), 4548−4551.

(7) Maeda, N.; Chen, N.; Tirrell, M.; Israelachvili, J. N. Adhesion and Friction Mechanisms of Polymer-on-Polymer Surfaces. *Science* **2002**, *297* (5580), 379−382.

(8) Chen, N.; Maeda, N.; Tirrell, M.; Israelachvili, J. N. Adhesion and Friction of Polymer Surfaces: The Effect of Chain Ends. *Macromolecules* **2005**, *38* (8), 3491−3503.

(9) Zeng, H.; Maeda, N.; Chen, N.; Tirrell, M.; Israelachvili, J. N. Adhesion and Friction of Polystyrene Surfaces around T G. *Macromolecules* **2006**, *39* (6), 2350−2363.

(10) Zeng, H.; Tirrell, M.; Israelachvili, J. N. Limit Cycles in Dynamic Adhesion and Friction Processes: A Discussion. *J. Adhes.* **2006**, *82* (9), 933−943.

(11) Zeng, H.; Zhao, B.; Israelachvili, J. N.; Tirrell, M. Liquid- to Solid-like Failure Mechanism of Thin Polymer Films at Micro- and Nanoscales. *Macromolecules* **2010**, *43* (1), 538−542.

(12) Faghihnejad, A.; Zeng, H. Hydrophobic Interactions between Polymer Surfaces: Using Polystyrene as a Model System. *Soft Matter* **2012**, *8* (9), 2746.

(13) Zeng, H.; Huang, J.; Tian, Y.; Li, L.; Tirrell, M.; Israelachvili, J. N. Adhesion and Detachment Mechanisms between Polymer and Solid Substrate Surfaces: Using Polystyrene-Mica as a Model System. *Macromolecules* **2016**, *49* (14), 5223−5231.

(14) Klein, J. The Interdiffusion of Polymers. *Science* **1990**, *250* (4981), 640−646.

(15) Chennevière, A.; Drockenmuller, E.; Damiron, D.; Cousin, F.; Boué, F.; Restagno, F.; Léger, L. Quantitative Analysis of Interdigitation Kinetics between a Polymer Melt and a Polymer Brush. *Macromolecules* **2013**, *46* (17), 6955−6962.

(16) Geoghegan, M.; Clarke, C. J.; Boué, F.; Menelle, A.; Russ, T.; Bucknall, D. G. The Kinetics of Penetration of Grafted Polymers into a Network. *Macromolecules* **1999**, *32* (15), 5106−5114.

(17) Lee, L.-H. Adhesion of High Polymers. I. Influence of Diffusion, Adsorption, and Physical State on Polymer Adhesion. *J. Polym. Sci. Part A-2 Polym. Phys.* **1967**, *5* (4), 751−760.

(18) Keddie, J. L.; Jones, R. A. L.; Cory, R. A. Interface and Surface Effects on the Glass-Transition Temperature in Thin Polymer Films. *Faraday Discuss.* **1994**, *98*, 219−230.

(19) Sharp, J. S.; Forrest, J. A. Free Surfaces Cause Reductions in the Glass Transition Temperature of Thin Polystyrene Films. *Phys. Rev. Lett.* **2003**, *91* (23), 235701.

(20) Fakhraai, Z.; Forrest, J. A. Measuring the Surface Dynamics of Glassy Polymers. *Science* **2008**, *319* (5863), 600−604.

DOI: 10.1021/acs.langmuir.9b02037
Langmuir 2019, 35, 15674−15680

(21) Mansfield, K. F.; Theodorou, D. N. Molecular Dynamics Simulation of a Glassy Polymer Surface. *Macromolecules* **1991**, *24* (23), 6283−6294.
(22) Boiko, Y. M. Interdiffusion of Polymers with Glassy Bulk. *Colloid Polym. Sci.* **2011**, *289* (17−18), 1847−1854.
(23) Boiko, Y. M. Is Adhesion between Amorphous Polymers Sensitive to the Bulk Glass Transition? *Colloid Polym. Sci.* **2013**, *291* (9), 2259−2262.
(24) Israelachvili, J. N.; Min, Y.; Akbulut, M.; Alig, A.; Carver, G.; Greene, W.; Kristiansen, K.; Meyer, E.; Pesika, N.; Rosenberg, K.; Zeng, H. Recent Advances in the Surface Forces Apparatus (SFA) Technique. *Rep. Prog. Phys.* **2010**, *73* (3), 036601.
(25) Israelachvili, J. N.; Alcantar, N. A.; Maeda, N.; Mates, T. E.; Ruths, M. Preparing Contamination-Free Mica Substrates for Surface Characterization, Force Measurements, and Imaging. *Langmuir* **2004**, *20*, 3616.
(26) *Physical Properties of Polymers Handbook*; Mark, J. E., Ed.; Springer, 2007.
(27) Bailey, A. I.; Kay, S. M. Measurement of Refractive Index and Dispersion of Mica, Employing Multiple Beam Interference Techniques. *Br. J. Appl. Phys.* **1965**, *16* (1), 39−44.
(28) Keddie, J. L.; Jones, R. A. L.; Cory, R. A. Size-Dependent Depression of the Glass Transition Temperature in Polymer Films. *EPL* **1994**, *27* (1), 59−64.
(29) Tabor, D. Surface Forces and Surface Interactions. *J. Colloid Interface Sci.* **1977**, *58* (1), 2−13.
(30) Derjaguin, B. V.; Muller, V. M.; Toporov, Y. P. Effect of Contact Deformations on the Adhesion of Particles. *J. Colloid Interface Sci.* **1975**, *53* (2), 314−326.
(31) McGuiggan, P. M.; Wallace, J. S.; Smith, D. T.; Sridhar, I.; Zheng, Z. W.; Johnson, K. L. Contact Mechanics of Layered Elastic Materials: Experiment and Theory. *J. Phys. D: Appl. Phys.* **2007**, *40* (19), 5984−5994.
(32) Zhang, G.; Wei, Z.; Ferrell, R. E.; Guggenheim, S.; Cygan, R. T.; Luo, J. Evaluation of the Elasticity Normal to the Basal Plane of Non-Expandable 2:1 Phyllosilicate Minerals by Nanoindentation. *Am. Mineral.* **2010**, *95* (5−6), 863−869.
(33) Christensen, N. I. Poisson's Ratio and Crustal Seismology. *J. Geophys. Res.* **1996**, *101* (B2), 3139−3156.
(34) Wool, R. P.; O'Connor, K. M. Craze Healing in Polymer Glasses. *Polym. Eng. Sci.* **1981**, *21* (14), 970−977.
(35) Prager, S.; Tirrell, M. The Healing Process at Polymer-Polymer Interfaces. *J. Chem. Phys.* **1981**, *75* (10), 5194−5198.
(36) Gent, A. N.; Lai, S.-M. Adhesion and Autohesion of Rubber Compounds: Effect of Surface Roughness. *Rubber Chem. Technol.* **1995**, *68* (1), 13−25.
(37) Padhye, N.; Parks, D. M.; Trout, B. L.; Slocum, A. H. A New Phenomenon: Sub-T g, Solid-State, Plasticity-Induced Bonding in Polymers. *Sci. Rep.* **2017**, *7*, 46405.
(38) Barus, C. Isothermals, Isopiestics and Isometrics Relative to Viscosity. *Am. J. Sci.* **1893**, *45* (266), 87−96.
(39) Kadijk, S. E.; Van Den Brule, B. H. A. A. On the Pressure Dependency of the Viscosity of Molten Polymers. *Polym. Eng. Sci.* **1994**, *34* (20), 1535−1546.
(40) Sedlacek, T.; Zatloukal, M.; Filip, P.; Boldizar, A.; Saha, P. On the Effect of Pressure on the Shear and Elongational Viscosities of Polymer Melts. *Polym. Eng. Sci.* **2004**, *44* (7), 1328−1337.
(41) Reynolds, C.; Thompson, R.; Mcleish, T. *J. Rheol.* **2018**, *62*, 631−642.
(42) Ruths, M.; Granick, S. Rate-Dependent Adhesion between Polymer and Surfactant Monolayers on Elastic Substrates. *Langmuir* **1998**, *14* (7), 1804−1814.
(43) Horn, R. G.; Israelachvili, J. N.; Pribac, F. Measurement of the Deformation and Adhesion of Solids in Contact. *J. Colloid Interface Sci.* **1987**, *115* (2), 480−492.
(44) Rubinstein, M.; Colby, R. H. *Polymer Physics*; Oxford University Press, 2003.
(45) Fetters, L. J.; Lohse, D. J.; Colby, R. H. Chain Dimensions and Entanglement Spacings. In *Physical Properties of Polymers Handbook*; Springer: New York, 2007; pp 447−454.

DOI: 10.1021/acs.langmuir.9b02037
Langmuir 2019, 35, 15674−15680